

Optical interactions in a plasmonic particle coupled to a metallic film

Gaëtan Lévêque and Olivier J. F. Martin

*Nanophotonics and Metrology Laboratory
Swiss Federal Institute of Technology Lausanne
EPFL-STI-NAM, ELG Station 11
CH-1015 Lausanne, Switzerland
gaetan.leveque@epfl.ch*

<http://www.nanophotonics.ch/>

Abstract: The interplay between localized surface plasmon (LSP) and surface plasmon-polariton (SPP) is studied in detail in a system composed of a three-dimensional gold particle located at a short distance from a gold thin film. Important frequency shifts of the LSP associated with the particle are observed for spacing distances between 0 and 50 nm. Beyond this distance the LSP and SPP resonances overlap, although some cavity effects between the particle and the film can still be observed. In particular, when the spacing increases the field in the cavity decreases more slowly than one would expect from a simple image dipole interpretation. For short separations the coupling between the particle and the film can produce a dramatic enhancement of the electromagnetic field in the space between them, where the electric field intensity can reach 5000 times that of the illumination field. Several movies show the spectral and time evolutions of the field distribution in the system both in and out of resonance. The character of the different modes excited in the system is studied. They include dipolar and quadrupolar modes, the latter exhibiting essentially a magnetic response.

© 2006 Optical Society of America

OCIS codes: (240.6680) Surface Plasmons; (260.3910) Optics of metals; (130.3120) Integrated optics devices

References and links

1. K. Kneipp, and H. Kneipp, "Surface enhanced Raman scattering - A tool for ultrasensitive trace analysis," *Can. J. Anal. Sci. Spectrosc.* **48**, 125-131 (2003).
2. A. Rasmussen, and V. Deckert, "Surface- and tip-enhanced Raman scattering of DNA components," *J. Raman Spectrosc.* **37**, 311-317 (2006).
3. A. V. Whitney, J. W. Elam, S. L. Zou, A. V. Zinovev, P. C. Stair, G. C. Schatz, and R. P. Van Duyne, "Localized surface plasmon resonance nanosensor: A high-resolution distance-dependence study using atomic layer deposition," *J. Phys. Chem. B* **109**, 20522-20528 (2005).
4. J. Seidel, S. Grafstrom, and L. Eng, "Stimulated emission of surface plasmons at the interface between a silver film and an optically pumped dye solution," *Phys. Rev. Lett.* **94**, 177401 (2005).
5. P. Berini, R. Charbonneau, N. Lahoud, and G. Mattiussi, "Characterization of long-range surface-plasmon-polariton waveguides," *J. Appl. Phys.* **98**, 043109 (2005).
6. J. P. Kottmann, O. J. F. Martin, D. R. Smith, and S. Schultz, "Plasmon resonances of silver nanowires with a nonregular cross section," *Phys. Rev. B* **64**, 235402 (2001).
7. S. I. Bozhevolnyi, J. Erland, K. Leosson, P. M. W. Skovgaard, and J. M. Hvam, "Waveguiding in surface plasmon polariton band gap structures," *Phys. Rev. Lett.* **86**, 3008 (2001).

8. I. P. Radko, T. Sondergaard, S. I. Bozhevolnyi, "Adiabatic bends in surface plasmon polariton band gap structures," *Opt. Express* **14**, 4107 (2006).
9. J.-C. Weeber, Y. Lacroute, A. Dereux, E. Devaux, T. Ebbesen, C. Girard, M. U. González, and A.-L. Baudrion, "Near-field characterization of Bragg mirrors engraved in surface plasmon waveguides," *Phys. Rev. B* **70**, 235406 (2004).
10. J.-C. Weeber, M. U. González, A.-L. Baudrion, and A. Dereux, "Surface plasmon routing along right angle bent metal strips," *App. Phys. Lett.* **87**, 221101 (2005).
11. W. L. Barnes, A. Dereux, and T. W. Ebbesen, "Surface plasmon subwavelength optics," *Nature* **424**, 824 (2003).
12. V. S. Volkov, S. I. Bozhevolnyi, E. S. Devaux, T. W. Ebbesen, "Compact gradual bends for channel plasmon polaritons," *Opt. Express* **14**, 4494-4503 (2006).
13. W. R. Holland, and D. G. Hall, "Frequency Shifts of an Electric-Dipole Resonance near a Conducting Surface," *Phys. Rev. Lett.* **52**, 1041 (1984).
14. M. Paulus, and O. J. F. Martin, "Light propagation and scattering in stratified media: a Green's tensor approach," *J. Opt. Soc. Am. A* **18**, 854 (2001).
15. J. P. Kottmann, and O. J. F. Martin, "Accurate Solution of the Volume Integral Equation for High-Permittivity Scatterers," *IEEE Trans. Antennas Propagat.* **48**, 1719 (2000).
16. P. B. Johnson and R. W. Christy, "Optical constants of the noble metals," *Phys. Rev. B* **6**, 4370 (1972).
17. B. T. Draine, "The discrete dipole approximation and its application to interstellar graphite grains," *Astrophys. J.* **333**, 848 (1988).
18. G. Dolling, C. Enkrich, M. Wegener, C. M. Soukoulis, and S. Linden, "Simultaneous Negative Phase and Group Velocity of Light in a Metamaterial," *Science* **312**, 892-894 (2006).

1. Introduction

Over the last few years there has been a surge in the interest for surface plasmon optics. The extremely strong and localized electromagnetic fields generated in such metallic systems open fascinating applications in chemistry [1, 2], sensing [3], and optical signal processing at the nanoscale [4, 5].

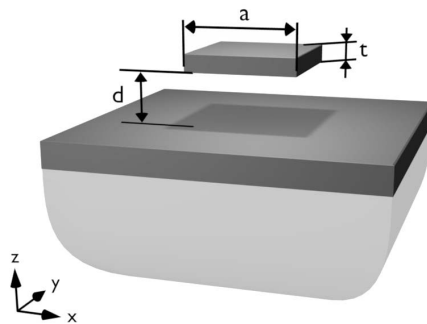


Fig. 1. Geometry of the system investigated: a square-basis gold particle of thickness t and side a is located at a distance d above a 50-nm-thick gold film deposited on a silica substrate.

Plasmonics relies on the excitation of electromagnetic modes associated to collective oscillations of the electronic charge density in the metal. These electromagnetic modes manifest differently depending whether the metallic system is localized or delocalized. Localized surface plasmon (LSP) modes are associated with a small metallic particle of subwavelength dimensions and are non dispersive. They depend on the particle geometry, material and environment [6]. LSP are often associated with a large enhancement of the electric field, generally localized at sharp corners of the particle. Delocalized surface plasmon modes, or surface plasmon-polariton (SPP) modes are surface waves confined near a metal-dielectric interface, which can

propagate over large distances (around 5 to 10 μm for gold in visible). SPP can be laterally confined using a metallic stripe, a band-gap structure [7, 8], a nanowire of subwavelength section [9, 10, 11], or a channel dug inside a metal film [12].

In this article we investigate the coupling and the interplay between LSP and SPP by studying the interaction between a three-dimensional gold nanoparticle and a thin gold film deposited on a silica substrate (Fig. 1). This system supports a delocalized and a localized surface plasmon mode. Furthermore, the localized resonance associated to the particle strongly depends on the distance between the particle and the layer [13]. Extinction spectra, far-field spectra and movies showing the evolution of the electric field with wavelength and time are presented. Calculations have been done using the Green's tensor method described in Refs. [14, 15].

The system under study is a square-basis gold particle separated from a gold thin film by an air gap of thickness d (Fig. 1). The side of the particle is a and its thickness t . The gold film is 50-nm thick and lies on a glass substrate with permittivity $\epsilon = 2.25$. The whole system is illuminated through the glass by a plane wave propagating in the xz -plane. Its angle with the interface normal is 45° and its polarization is p . Throughout the article, the width of the particle is $a = 110$ nm and its thickness is $t = 50$ nm. The gold permittivity data are from P. B. Johnson and R. W. Christy [16].

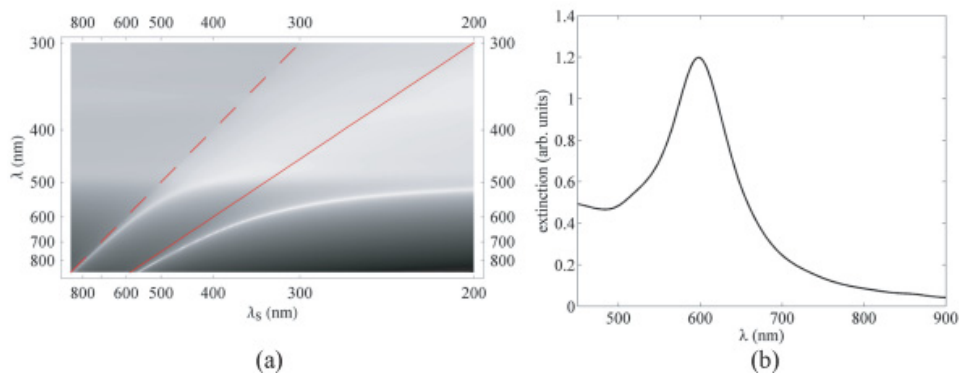


Fig. 2. (a) Dispersion curve of the SPP modes established at the two interfaces of a 50-nm-thick gold slab deposited on a glass substrate. The red lines represent the light lines of the air (dashed) and the glass (solid). Axes are the inverse surface wavelength (horizontal axis), and the inverse free-space wavelength (vertical axis). (b) Extinction spectrum of the gold particle in free space.

2. Individual systems

The dispersion relation of the SPP for the substrate-gold slab system without particle is shown in Fig. 2(a). One surface wave can propagate on each interface. The two red lines in Fig. 2(a) represent the light-lines associated with the dielectrics on each side of the metal. Only the mode whose curve lies above the glass light-line can be excited. No surface plasmons wave can propagate for a wavelength smaller than 500 nm, which is roughly the asymptotic value of the air/metal dispersion curve. For an incidence angle of 45° the SPP is excited at a wavelength of $\lambda = 600$ nm. The corresponding SPP wavelength is $\lambda_s = \lambda / (n \sin(45^\circ)) = 566$ nm, where n is the substrate index. Figure 2(b) shows the extinction spectrum of the gold particle in the air, without substrate or metallic film. The extinction coefficient is computed from the field in the particle, as explained in Ref. [17]. Figure 2(b) shows that the LSP resonance is located at $\lambda = 600$ nm. The geometry of the illumination is the same as in the global system, *i.e.* the

incidence angle is 45° . Two resonances should appear, one for the long edge of the particle and the other one for the short edge. The surface plasmon frequency of an infinitely small gold particle with spherical shape is given by $\epsilon(\lambda) = -2$, which arises around $\lambda = 490$ nm for gold. Hence, the second resonance should be larger than this value, since it is red-shifted when the volume of the particle increases. Actually the second peak is located in the blue-tail of the plasmon resonance and is not observable because of the large absorption of gold which broadens the resonance peak. This fact appears clearly on the following time varying analysis of the electric field at the resonance wavelength.

The movie corresponding to Figs. 3(a) and (b) shows the time evolution of the amplitude and polarization of the electric field in the incidence plane for the isolated particle, at the plasmon resonance frequency. The colorscale indicates the electric field amplitude normalized to the incident wave amplitude, and the green arrows indicate the projection of the electric field polarization $\mathbf{E}(\mathbf{r}, t)/|\mathbf{E}|$ on the incidence plane. The time evolution of the electric field is complex because it results from the interference of the incident field with the field scattered by the particle. When the field inside the particle is zero, which occurs when $t = 0.52T$ (Fig. 3(a)), where $T = 2\pi/\omega$ is the temporal period of light, the field outside the particle is similar to the incident wave: away from the particle, the electric field is parallel to a line which makes a -45° angle with the x -axis. Minima and maxima of the amplitude are mostly aligned parallel to the same line, which is consistent with a propagation of the wave along the corresponding perpendicular direction. At the edge of the particle, the electric field is perpendicular to the air/metal interface due to the strong permittivity contrast between the metal and air. The amplitude is maximum at the top-left and bottom-right corners and decreases rapidly away from the particle. This is a consequence of the tip effect which accumulates charges in the corners of the particle. Moreover, the opposite directions of the electric field show that the surface charges have opposite signs at these two corners: they are positive at the top-left corner (diverging arrows) and negative at the bottom-right corner (converging arrows). At a later time, the amplitude of the electric

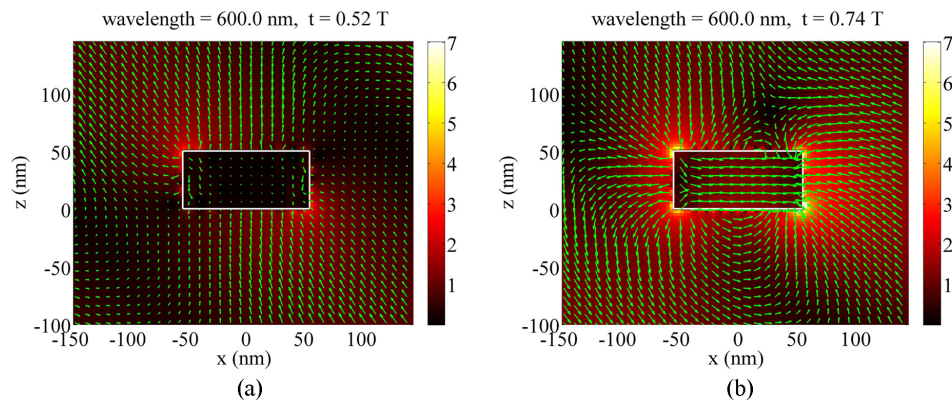


Fig. 3. Time evolution of the structure of the electric field inside the incidence plane at the plasmon resonance, $\lambda = 600$ nm. The colorscale represents the amplitude of the electric field and the green arrows represent the instantaneous direction of the projection of the polarization of the electric field on the incidence plane. (a) $t = 0.52T$; (b) $t = 0.74T$, where T is the temporal period of light. One movie of 2.6 Mb.

field increases a lot, first at the two top-left and bottom-right corners, while the electric field becomes maximum inside the particle. The maximum of the electric field inside the particle occurs at $t = 0.74T$ (Fig. 3(b)). At that instant, field is maximum and of similar amplitude near the four particle's corners. The direction of the electric field indicates that the surface charges

are positive on the left edge of the particle and negative on the right edge. This is consistent with the fact that the particle behaves mostly like a dipole oriented along its long side at the LSP resonance. The polarization pattern shows very well the interference between the incident and the scattered field. In the close vicinity of the particle the field lines reproduce the shape of the dipolar scattered field. But as the decay of the scattered field is fast (like $1/R^3$, where R is the distance to the center of the particle), its amplitude becomes rapidly equal to the one of the incident field. Hence, a destructive interference occurs inside the black area on the field map (around $x = 25$ nm, $z = 90$ nm on Fig. 3(b)) because the scattered and the incident field have opposite directions. On the other side of the particle, such a destructive interference does not appear because the phase of the incident field is different: the incident and the scattered field add constructively. Away from the particle, the linear polarization of the illumination field is recovered. Finally, for longer time, the bottom-left and top-right corners of the particle stay turned on longer than the two other corners. Actually, the delay between the two maxima for these two sets of opposed corners is around $\Delta t = 0.12T$, whereas the maximum of the field inside the particle is reached at the midtime between these two maxima. The explanation of this fact is that the short wavelength surface plasmon resonance is sufficiently near the long wavelength one to be excited by the diagonal illumination. The short-wavelength dipole (parallel to the z -axis) is phase shifted compared to the long-wavelength dipole (parallel to the x -axis), which implies a slightly elliptical resulting dipole inside the particle, mostly along the x -axis. This dipole will then excite with a phase delay the two corners pairs along the diagonal. This desynchronisation effect disappears when the particle is excited along the x - or z -direction.

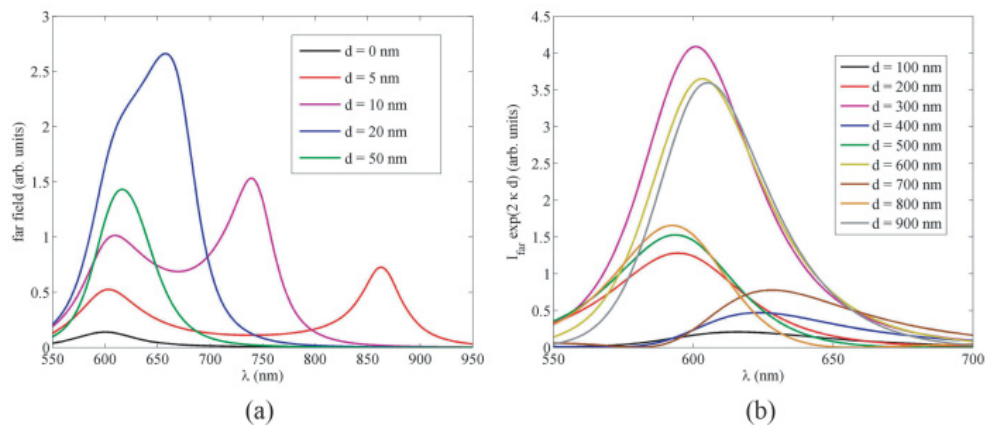


Fig. 4. Far-field spectrum of the gold particle for several distances d between the gold interface and the nanoparticle. The field intensity has been computed in the direction perpendicular to the surface, at infinity. (a) $d \leq 100$ nm; (b) for $d \geq 100$ nm, far-field intensities have been corrected by a factor $\exp(2\kappa d)$, $\kappa = 2\pi\sqrt{\epsilon \sin(45^\circ) - 1}/\lambda$ (see text).

3. Coupled systems

It is a well known fact that the resonance wavelength of such a particle depends on its shape, volume and environment [6, 13]. In particular, it is red-shifted when the dielectric constant of the surrounding dielectric increases. When approached towards a dielectric substrate, the plasmon resonance corresponding to the side parallel to the interface is shifted to the red [13]. This effect is even increased when the particle is approached towards a metallic interface. Figure 4(a) and (b) shows the far-field spectrum of the particle as a function of the distance d between the particle and the interface. The far-field was computed in the direction perpendicular to the

interface, at infinity. Two regimes can be identified: when the particle is in the near-field distance of the metallic layer ($0 \text{ nm} \leq d \leq 100 \text{ nm}$, Fig. 4(a)) and when the particle is further away (Fig. 4(b)). Two peaks appear in the near-field regime. A first peak occurs around 600 nm. Its position is almost independent of the distance d . It corresponds to the SPP mode propagating on the gold/air interface of the metallic film which is excited at this wavelength for an illumination angle of 45° . The corresponding enhancement of the particle excitation field increases the intensity of field scattered at infinity. A second peak is visible for $5 \text{ nm} \leq d \leq 20 \text{ nm}$: it corresponds to the LSP mode associated to the gold particle. It is rapidly shifted to large wavelengths when the distance d is decreased. When the separation is larger than 50 nm, the two peaks overlap. Figure 4(b) shows far-field spectrum for distances d larger than 100 nm. In order to take into account the decrease of the excitation field at the height of the particle, the intensity has been corrected by a factor $\exp(2\kappa d)$, where $\kappa = 2\pi\sqrt{\epsilon \sin(45^\circ) - 1}/\lambda$ is the vertical decay rate of the electromagnetic field. The reason is that the particle behaves as a transducer from evanescent to propagative wave, and that the intensity of the field detected at infinity is approximately proportional to the intensity of the illumination field in the particle. There is only one peak appearing in that range of wavelength (there are secondary peaks for some values of d above 700 nm but of much lower amplitude), which position changes with the spacing d (Fig. 4(b)). Additional calculations in which the metallic particle has been replaced by a dielectric particle have lead to roughly the same set of curves for $d \geq 100 \text{ nm}$, with very little difference, which tends to show that the LSP mode of the gold particle does not play a role in this oscillation. We can see that the corrected far-field intensity is the largest when the resonance occurs around 600 nm. Actually, this behaviour can be explained by the coupling of the SPP with the cavity formed by the particle and the film. Hence, when $d \approx m\lambda/2$, the cavity is tuned to the SPP wavelength and a large peak appears around 600 nm. If the distance is different, the plasmon mode can still be excited because the cavity is highly lossy, but its wavelength is shifted due to the partially destructive interferences which occur between the particle and the film.

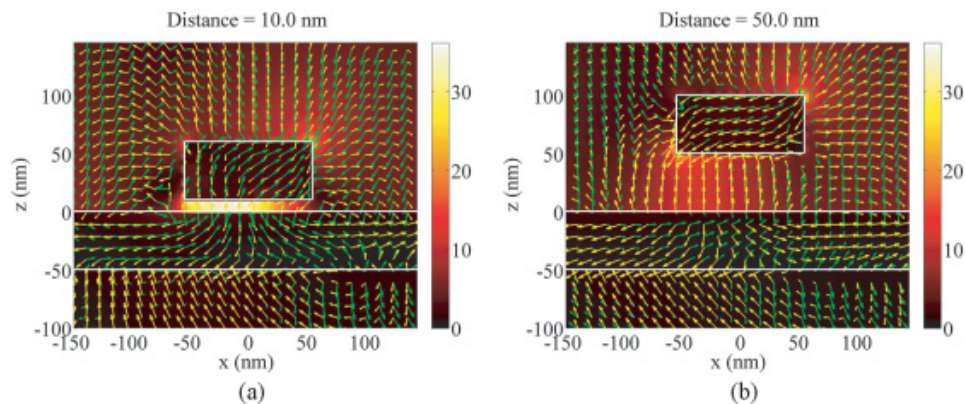


Fig. 5. Evolution of the structure of the electric field inside the incidence plane with the distance d between the gold film and the particle, at $\lambda = 600 \text{ nm}$. The colorscale represents the amplitude of the electric field. The green (respectively yellow) arrows represents the real (respectively imaginary) part of the electric field polarization. (a) $d = 10 \text{ nm}$; (b) $d = 50 \text{ nm}$. One movie of size 0.7 Mb.

The movie corresponding to Fig. 5(a) and (b) shows the evolution of the electric field amplitude (colorscale) and polarization when the particle grows from the layer, and when it moves away from the gold slab. The wavelength was fixed at the SPP wavelength $\lambda = 600 \text{ nm}$. The polarization of the electric field is indicated as a set of two arrows: the green one shows the

real part of the polarization vector, and the yellow one the imaginary part. In other words, the green arrow is the polarization at $t = 0T$ and the yellow arrow is the polarization at $t = 0.25T$. Hence, the polarization is linear when both arrows are aligned, otherwise it is elliptical. As long as the particle is in contact with the slab, the enhancement factor of the electric field intensity around the particle is weak. When the particle is only 10 nm thick, the SPP wave is almost not modified, as can be seen on the electric field polarization map which is very similar to the polarization map of the SPP without particle. Around $x = -140 \text{ nm} \approx -\lambda_s/4$, the real part of the polarization vector is normal to the interface and jabs upward. Around $x = 0 \text{ nm}$, it has turned by 45° in the clockwise direction. Around $x = 140 \text{ nm} \approx +\lambda_s/4$ the real part of the polarization points in the opposite direction than for $x = -\lambda_s/4$. The behavior is the same for the imaginary part, but with a phase shift of $\pi/2$. The polarization is only strongly modified inside the protusion. When the particle grows, the field lines become more and more distorted outside the particle because of the strong permittivity discontinuity imposed at its edges. In the same time, a complex structure of the polarization appears inside the metallic particle, while the intensity of the electric field is the highest on its sides. When the particle is not touching the metallic slab, the structure of the field is strongly modified compared to the previous case, as shown in Fig. 5. For short distances ($d \leq 50 \text{ nm}$), most of the energy is concentrated between

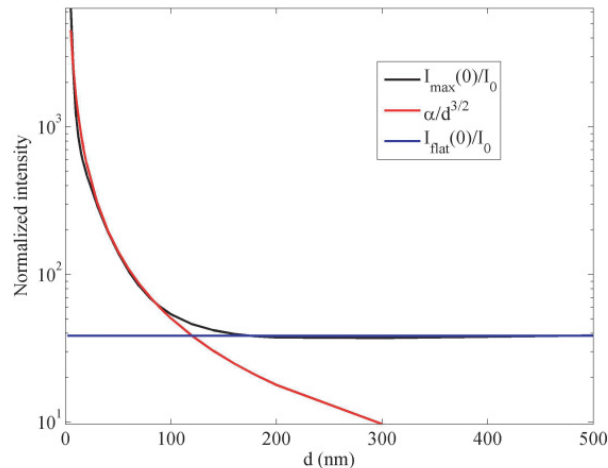


Fig. 6. Maximum intensity of the electric field along the top interface of the gold film as a function of the distance d between the particle and the layer (black line). The red line is a fit in $d^{-3/2}$, the blue line is the value of the electric field intensity just above the film without the metallic particle.

the particle and the film. When the distance d is about 10 nm (Fig. 5(a)), the intensity between the particle and the layer is about 1200 times the intensity of the incident field. For a very short separation this enhancement can even reach 5000; however, this value decreases rapidly when d increases (Fig. 5(b)). Figure 6 shows the maximum intensity of the electric field just above the metallic interface (black curve) as a function of the particle distance d . The red curve is a power law fit of these values which shows that the intensity between the particle scales almost perfectly like $d^{-3/2}$ between $d = 5 \text{ nm}$ and $d = 100 \text{ nm}$. This law is slower than what could be expected if we suppose that the field is the superposition of the incident field and a dipolar field radiated from the particle. In that case, the curve should behave like $\exp(-2\kappa d)/d^6$. This indicates that a strong charge effect occurs between the particle and the layer, which tends to

slow down the decrease of the field with the distance. For distances larger than 150 nm, the intensity is the value expected for a film without particle (Fig. 6, blue line).

The movies corresponding to Fig. 7(a) and (b) show the wavelength dependence of the amplitude and polarization of the electric field for the distances $d = 10$ nm and $d = 50$ nm. Following the curve of Fig. 4, we see that the two resonances associated with the two peaks of the $d = 10$ nm extinction spectrum have very specific electric field distributions. At the SPP wavelength $\lambda = 600$ nm, the polarization is perpendicular to the interface between the particle and the layer and the amplitude is mostly uniform in this area. Within the metallic layer, the polarization is linear and electric field lines flow from the particle bottom. At the LSP wavelength $\lambda = 740$ nm (Fig. 7(a)), the electric field is mainly concentrated at the bottom corners of the gold particle, and the polarization inside the particle indicates that the excited dipole is parallel to the interface. Hence the surface charges on each side of the particle are opposed. A node occurs in the middle of the space between the particle and the film. By influence, charges have the opposite

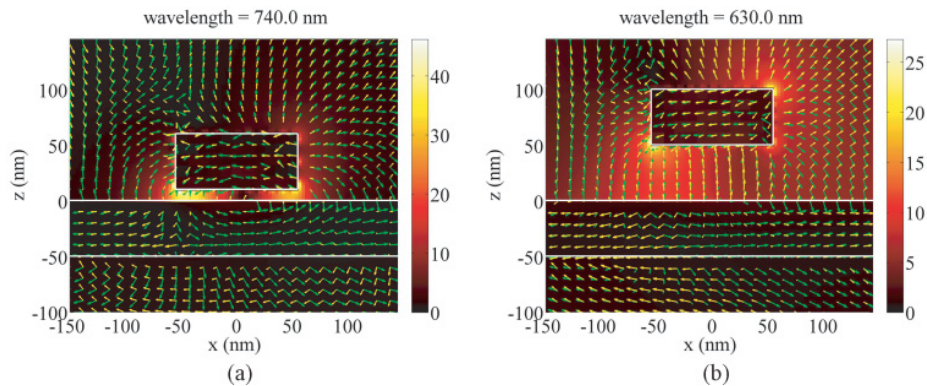


Fig. 7. Spectral evolution of the structure of the electric field inside the incidence plane for two distances between the gold layer and the particle: (a) $d = 10$ nm, (b) $d = 50$ nm. The colorscale represents the amplitude of the electric field. The green (respectively yellow) arrows represent the real (respectively imaginary) part of the electric field polarization. Two movies of size 1.7 Mb.

sign on the top film interface, which can be interpreted as the signature of the particle dipole image inside the layer, leading to a quadrupolar resonance. The red-shift of the resonance wavelength arises from the fact that the particle dipole is antisymmetrically coupled to its image inside the gold layer. For wavelengths larger than the LSP resonance wavelength, both the electric field polarization and the amplitude do no longer evolve significantly outside the object. For $d = 50$ nm, the two plasmon peaks are very close (Fig. 4(a)). But, if only one resonance is visible on the far field spectrum, the movie corresponding to Fig. 7(b) shows clearly two electric field distributions very similar to those observed for the SPP and LSP resonances for $d = 10$ nm. Indeed, for $\lambda \leq 610$ nm the intensity of the electric field increases under the particle and is mainly located around the top-right and bottom-left corners. Inside the particle, the electric field is mainly oriented along the corresponding diagonal. When the wavelength increases from 610 nm to 650 nm, the bottom-left corner begins to be light up, while the polarization of the electric field aligns along the x -axis. At $\lambda = 660$ nm, the field distribution looks like that at $\lambda = 740$ nm for the case $d = 10$ nm (compare the movies in Figs. 7(a) and (b)). For $\lambda \geq 660$ nm the intensity of the electric field decreases. Finally, the electric field remains normal to the interface between the object and the film because of the strong discontinuity of the permittivity between metal and air. Hence, the study of the electric field distributions shows that within the

broad peak around 600 nm in Fig. 4(a) the particle response evolves from mainly SPP to mainly LSP, in a few tens of nanometers.

We will in the following focus on the case of a $d = 10$ nm spacing and study the field generated in the gap between the particle and the film. The movie corresponding to Fig. 8(a) and (b) shows the evolution of the electric field amplitude and polarization as a function of the illumination wavelength just above the metallic interface. At $\lambda = 600$ nm (Fig. 8(a)), the electric

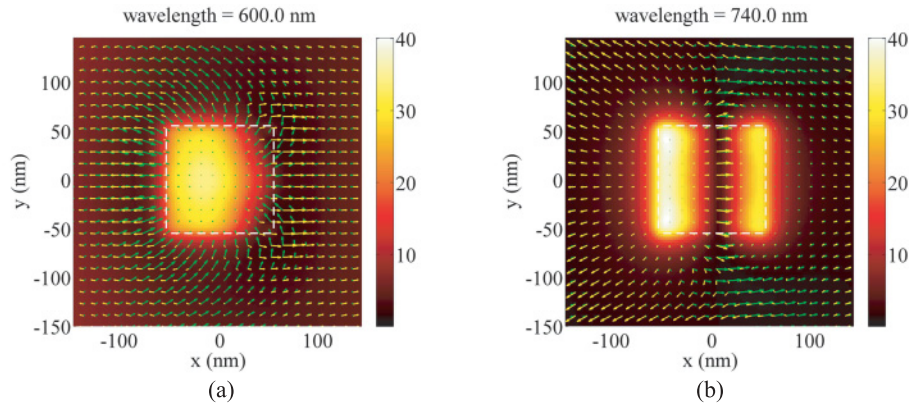


Fig. 8. Spectral evolution of the structure of the electric field in the gap between the particle and the film, just above the metallic film ($z = 0^+$) for a distance between the gold film and the particle of $d = 10$ nm. The colorscale represents the amplitude of the electric field. The green (respectively yellow) arrows represent the real (respectively imaginary) part of the electric field polarization. (a) $\lambda = 600$ nm; (b) $\lambda = 740$ nm. One movie of size 1.6 Mb.

field is perpendicular to the top interface of the metallic layer under the particle. The real part of the polarization, which corresponds to the direction of the electric field at $t = 0T$, shows that the field scattered by the particle in the xy -plane has a dipolar shape. The projection of the corresponding dipole on the xy -plane is aligned along the x -direction. The left/right dissymetry of the field lines arises from the interference between the incident and the scattered field. The imaginary part of the polarization is very different as it is almost perfectly aligned along the x -axis. This indicates that at $t = T/4$, the particle is “off”, the scattered field being then zero, and the total field is simply equal to the incident field. Moreover, we can see that the electric field is still strongly localized under the particle 10 nm away from it, and that the intensity enhancement factor is about 1200. At $\lambda = 740$ nm (Fig. 8(b)), the electric field has a strong parallel component along the x -axis at the center of the particle, but it is normal to the interface along its left and right edges. This shows that field lines form closed loops around the separation between the particle and the metallic film. This resonance is then mainly of magnetic nature and may play a key role for creating negative refraction in such a system [18]. The electric field intensity enhancement factor is about 1400. It is larger on the left edge of the particle, where the SPP is reflected, than on the right edge.

Finally, Fig. 9 shows three movies that display the time evolution of the instantaneous amplitude and polarization of the electric field for $d = 10$ nm, at different excitation wavelengths. The first one is out of resonance: $\lambda = 500$ nm (Fig. 9(a)). The field is only enhanced at the corners of the gold particle. The time evolution of the electric field between the particle and the gold layer is not stationary, the field minimum travels from left to right, following the propagation direction of the incident wave which is visible at the top of the figure. The situation is different at $\lambda = 610$ nm (Fig. 9(b)), where the electric field between the particle and the film is essentially stationary. The field increase is simultaneous in the interspace and at the top-right

corner of the particle. Its maximum coincides with the alignment of the internal electric field along the diagonal of the particle section. Moreover, we can see that the surface charges are of opposite sign at the bottom edge and top-right corner of the particle. For example, the amplitude is maximal at $t = 0.34T$, the surface charge is then positive along the top and right edges and negative along the bottom edge. This is a consequence of the fact that the electric field inside the particle oscillate along the diagonal. For $\lambda = 740$ nm (Fig. 9(c)), the field inside the particle oscillates parallel to the layer. The electric field evolution remains stationary between the particle and the film. Contrary to the case $\lambda = 610$ nm, the surface charge has opposite signs on the left and right edges, as can be seen for example at $t = 0.52T$, which corresponds to the maximum field intensity. Surface charge is then positive along the left edge and negative along the right edge. Along the bottom edge, the surface charge evolves from positive on the left to positive on the right.

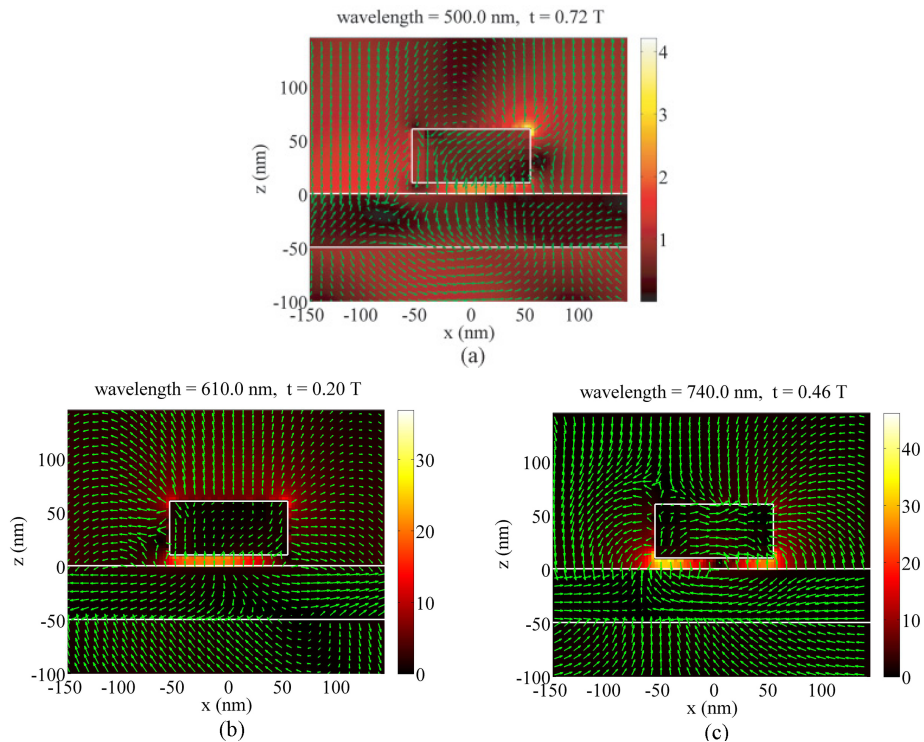


Fig. 9. Time evolution of the structure of the electric field inside the incidence plane for $d = 10$ nm and for three wavelengths: (a) $\lambda = 500$ nm, (b) $\lambda = 610$ nm, and (c) $\lambda = 740$ nm. The colorscale represents the amplitude of the electric field, and the green arrows represent the instantaneous direction of the projection of the polarization of the electric field on the incidence plane. Three movies of size 2.7 Mb.

4. Summary

We have studied in details the interplay between localized surface plasmon (LSP) and surface plasmon-polariton (SPP) in a system composed of a gold particle coupled to a gold thin film. Several movies have highlighted the coupling mechanisms between the particle and the thin gold film. The properties of this system are controlled by the space between the particle and the layer, which strongly changes the position of the LSP mode associated to the particle. The peak

associated to the SPP mode is essentially not displaced in the near field interaction region, that is when the distance between the particle and the film is smaller than 100 nm. For larger distances, the SPP mode is coupled to the highly lossy cavity formed by the particle and the film, which produces a slight shift of the SPP resonance wavelength of some tens of nanometers. The diminution of the distance d below 50 nm shifts the LSP to the red. The higher enhancement of the intensity occurs for distances smaller than 10 nm. In that case, the LSP and SPP modes are well separated in wavelength, and they are characterized by very different electric field distribution, both in amplitude and polarization. The resonance at the SPP wavelength is characterized by a uniform electric field aligned along the vertical direction in the space between the particle and the film, while the LSP resonance has a strong quadrupolar character, originating in the antisymmetric coupling between the particle dipole along the x -axis and its image in the metal. Moreover, we have seen that the field along the interface reaches its maximum under the particle and follows a law in $d^{-3/2}$ with the distance between the particle and the film. This shows that a strong charge effect occurs in this region of the system. Finally, we observed an electric field intensity enhancement of 5000 for the LSP resonance $\lambda = 610$ nm in the case $d = 5$ nm.

Acknowledgments

Authors acknowledge fruitful discussions with professor S. A. Ramakrishna from Indian Institute of Technology Kanpur, India, and funding from the IST Network of Excellence Plasmonanodevices (FP6-2002-IST-1-507879).